Microporous and Mesoporous Materials 331 (2022) 111659

Contents lists available at ScienceDirect

Microporous and Mesoporous Materials

journal homepage: www.elsevier.com/locate/micromeso

Computational screening of metal-organic frameworks for ammonia capture from humid air

Zhilu Liu [a,1], Xinbo Wang [b,1], Yuexin Liu [a], Li Li [b,**], Song Li [a,*]

[a] School of Energy and Power Engineering, Huazhong University of Science and Technology, Wuhan, 430074, China
[b] State Key Laboratory of NBC Protection for Civilian, Research Institute of Chemical Defense, Beijing, 100191, China

ARTICLE INFO

Keywords:
Grand canonical Monte Carlo simulations
Hydrophilic
Ammonia uptake
Selectivity
Adsorption competition

ABSTRACT

Metal-organic frameworks (MOFs) are potential adsorbents for ammonia capture. However, exploration of high-performing MOFs for ammonia adsorption from humid air is still challenging due to the competitive adsorption between ammonia and water molecules. In this work, high-throughput computational screening of 2932 CoRE MOFs for ammonia capture from humid air was carried out by grand canonical Monte Carlo (GCMC) simulations. It was found that the affinities or Henry's constant of MOFs towards ammonia and water molecules play a more important role in determining the ammonia capture performance than their structural properties. Hydrophobic MOFs exhibited higher ammonia selectivity, while hydrophilic MOFs possessed higher ammonia uptake regardless of the strong adsorption competition from water molecules. The coefficient describing the impacts of water adsorption on ammonia uptake (IC_{H2O_NH3}) revealed that although water adsorption promoted the ammonia uptake in the MOFs with $IC_{H2O\_NH3} < 0$, their ammonia uptake is still lower than that with $IC_{H2O\_NH3} > 0$ due to their ultra-low affinity towards ammonia. Moreover, analysis of top performers from screening demonstrated that the competitive adsorption between ammonia and water can be identified by their similar density and potential energy distributions of adsorbed ammonia and water molecules.

1. Introduction

Ammonia (NH_3) is a colorless, pungent, toxic and corrosive gas, which belongs to the class of toxic industrial chemicals (TICs) and is regarded as the most important gaseous alkaline pollutant [1–3]. Exposure to > 50 ppm (i.e. 34.76 μg/L) ammonia can lead to temporary blindness and pulmonary edema, and it will cause irreversible effects and even death at a concentration of 500 ppm (i.e. 347.65 μg/L) [2,4]. As for personnel involved in industrial operations and military activities, efficient protective equipments such as gas masks with filter cartridges are required for the removal of ammonia from air [2,5]. Metal-organic frameworks (MOFs) are crystalline nanoporous materials assembled from metal nodes and organic linkers [6], which possesses unique advantages such as high surface area, high porosity, controllable pore size and tunable pore surface [7,8], and thus has been widely used in gas adsorption, photocatalysis and catalysis [9–11]. Ammonia capture by MOFs [12] has won the growing research interest due to their ultra-high surface area, pore volume and structural diversity that are favorable for selective gas adsorption. It has been reported that Zr-based MOFs such as functional UiO-66 [5,13] and NU-300 [14] exhibit an ammonia uptake of ~10 mmol/g at an ammonia pressure of 1 bar and 298 K Mn_2Cl_2BTDD [15] and Cu_2Cl_2BBTA [16] have high ammonia uptakes of 15.47 mmol/g and 19.79 mmol/g, respectively, at 1 bar. Very recently, Mg_2(dobpdc) [17] was reported to possess a record-breaking ammonia uptake of 23.9 mmol/g at the ammonia pressure of 1 bar and 298 K, outperforming other solid adsorbents such as zeolites and carbon.

However, ammonia capture by MOFs from air, especially from humid air is a challenging task due to its trace amount in atmosphere and the possible detrimental effects of water molecules in humid air on frameworks. It has been reported that MOFs with Lewis acidic open metal sites such as CuBTC [18–20] and M-MOF-74 (M = Cu, Mg, Co, Ni and Zn) [21,22] are potential candidates for ammonia capture from air. It is found that CuBTC exhibits an ammonia uptake of 2.8 mmol/g under dry air and 1.9 mmol/g under humid air with a relative humidity (RH) of 80% by breakthrough measurement, which is ascribed to the irreversible structure and porosity loss under humid conditions [20]. In addition, the

* Corresponding author.
** Corresponding author.
E-mail addresses: lily97@buaa.edu.cn (L. Li), songli@hust.edu.cn (S. Li).
[1] These authors contributed equally to this work.

https://doi.org/10.1016/j.micromeso.2021.111659
Received 25 October 2021; Received in revised form 24 December 2021; Accepted 24 December 2021
Available online 28 December 2021

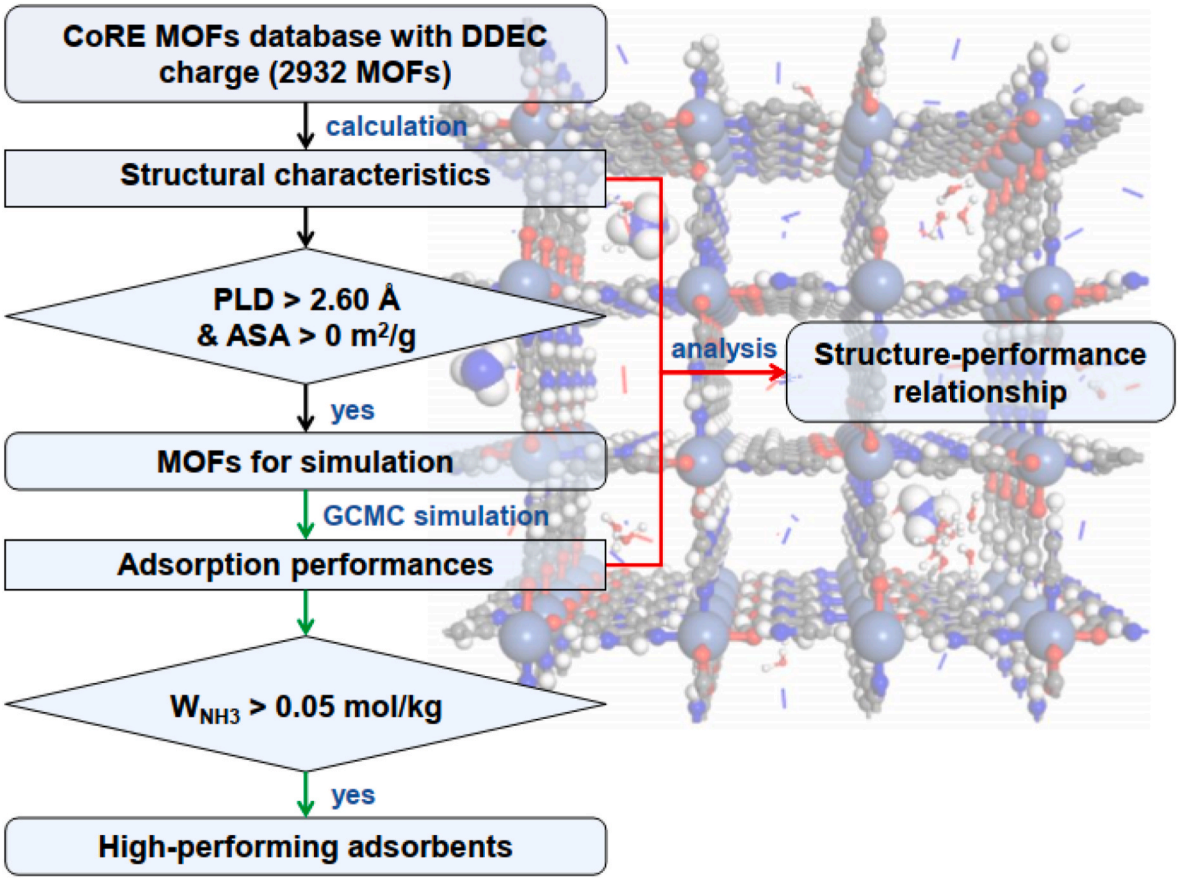

Fig. 1. Schematic diagram of the computational screening strategy for ammonia capture from humid air.

ammonia capture performance of 18 MOFs under dry and humid air (40% RH, 1200 ppm (i.e. 934.36 μg/L) ammonia) has been tested by breakthrough measurement [2], in which the ammonia uptakes of most MOFs are increasing at humid conditions, and the dependence of ammonia uptake on water uptake of these MOFs is ascribed to the enhanced solubilization of ammonia in water.

All the abovementioned experimental studies were focused on a limited number of MOFs. With the rapidly increasing number of MOFs, there is an urgent need to identify high-performing candidates from a vast number of MOFs for ammonia capture from humid air. High-throughput computational screening (HTCS) based on grand canonical Monte Carlo (GCMC) simulations has been used to accelerate the exploitation of top-performing MOFs and relevant structure-performance relationship (SPR) [23,24]. Moghadam et al. [25] conducted HTCS of hypothetical MOFs (hMOFs) for ammonia capture (290 ppm = 201.64 μg/L) from humid air at 298 K and 80% RH. Given the adsorption competition between water and ammonia molecules as well as the detrimental effects of humidity on frameworks, their screening is focused on 2777 hydrophobic MOFs which possessed high ammonia selectivity over water molecules. Although the hydrophobic MOFs with high ammonia selectivity were selected through HTCS, no MOFs with satisfactory ammonia uptake were identified until increasing the ammonia content up to 10,000 ppm (i.e. 6952.97 μg/L). In special applications such as protective equipment used in military activities, the high ammonia uptake is a greater concern compared with ammonia selectivity. One question arising is that whether the hydrophilic MOFs should be taken into account to identify top performers with high ammonia uptakes. Another question is how the hydrophilicity of MOFs affects their ammonia uptake from humid air. In this work, a different HTCS strategy that concentrated on the ammonia uptake from humid air was adopted. Considering the synthesizability of MOFs, we carried out a HTCS of Computation-Ready, Experimental (CoRE) MOFs consisting of 2932 structures regardless of their hydrophilicity for ammonia capture from humid atmosphere, and analyzed the relationships between structural characteristics, hydrophilicity and ammonia uptake.

2. Methods

The schematic diagram of the screening procedure was presented in Fig. 1. The ammonia capture performance from the humid air by 2932 MOFs from the CoRE MOF database [26] was evaluated. After the pre-screening to exclude the structures with inaccessible pores for ammonia, screening based on GCMC simulations was carried out from which the high-performing candidates with ammonia uptake $>$ 0.05 mol/kg were identified. Based on the calculated structural characteristics, adsorption properties and adsorption performance from GCMC simulations, the structure-performance relationship (SPR) was also obtained.

2.1. MOF database for screening

The CoRE MOF database has been widely used for calculation and screening in gas adsorption [27,28] and separation [29,30]. It has been reported that the electrostatic potential plays a dominant role in describing the interaction between MOFs and polar gases such as ammonia and water molecules [31]. The precise atomic charge of MOFs can more accurately describe the electrostatic interactions, hence 2932 CoRE MOFs with high-precision Density Derived Electrostatic and Chemical (DDEC) charge [32] were chosen for GCMC simulations of ammonia capture from the humid air.

To enhance the screening efficiency, the pre-screening based on the structural characteristics was carried out before GCMC simulation. The

Table 1
Separation conditions of GCMC simulations for ammonia capture from humid air.

Conditions	Ammonia and humid air			
Temperature (K)	298			
Pressure (Pa)	100000			
Components and molar ratio	N_2	O_2	NH_3 (1000 ppm = 695.3 μg/L)	H_2O (80% RH)
	0.76912	0.19228	0.001	0.0376

structural characteristics including pore limiting diameter (PLD), largest cavity diameter (LCD), accessible surface area (ASA) and available pore volume (V_a) were calculated using Zeo++ 0.3 [33]. The detailed data was provided in Table S1 of Supporting Information (SI). The crystal structures with PLD less than 2.60 Å (i.e. the dynamic diameter of ammonia molecule) and ASA equal to zero were removed, and the remained 1709 MOFs were selected for GCMC simulations. In addition, Henry's constant (K_H) that describes the hydrophilicity of the adsorbents were computed for 1709 MOFs at 298 K using Widom insertion method by RASPA 2.0 [34], which was provided in Table S2.

2.2. Grand canonical Monte Carlo simulation

GCMC simulation was carried out for 1709 MOFs to obtain their gas adsorption information using RASPA 2.0 [34]. It should be noted that the reversible physical adsorption is not required for adsorbents of one-off protective equipment in military activities. Thus, MOFs are assumed stable during physical adsorption process and all atoms of MOFs are frozen in GCMC simulations. In the simulation, the interactions between MOFs and adsorbate molecules are described by van der Waals potential and coulombic term (Eq. (1)).

$$U_{ij} = 4\varepsilon_{ij}\left[\left(\frac{\sigma_{ij}}{r_{ij}}\right)^{12} - \left(\frac{\sigma_{ij}}{r_{ij}}\right)^{6}\right] + \frac{q_i q_j}{4\pi\varepsilon_0 r_{ij}} \quad \text{(Eq. 1)}$$

Where i and j represent the interacting atoms, r_{ij} is the distance between atoms i and j, ε is the depth of potential well, and σ is the equilibrium position of potential energy, q is the atomic charge, and ε_0 is the vacuum permittivity constant. The Lennard-Jones (LJ) parameters were adopted from the universal force field (UFF) [35] and DDEC charge [32] were adopted for all atoms of the MOFs. All adsorbate molecules including nitrogen, oxygen, ammonia and water were described by Transferable Potentials for Phase Equilibria (TraPPE) force field parameters [36] in Table S5. The van der Waals potential was described by 12-6 LJ expression with the Lorentz Berthelot mixing rule for interatomic interactions. A spherical cutoff of 14 Å and analytic tail correction were used for the Lennard-Jones interactions. The long-range electrostatic interaction was handled using the Ewald summation technique.

As for each cycle in GCMC simulations, five types of Monte Carlo moves with equal probability were implemented, including translation, rotation, insertion, deletion and reinsertion. In order to reduce computational costs and improve screening efficiency, we adopted the three-round screening strategy whose accuracy and efficiency have been proved in previous work [28]. In the first round, 1×10^4 Monte Carlo cycles including 5×10^3 cycles for equilibration and 5×10^3 cycles for production were used to estimate the gas adsorption performance, and the results were used to obtain the SPR between structural characteristics, adsorption properties and adsorption performance. Then, the MOFs with ammonia adsorption capacity (W_{NH3_hum}) greater than 0.05 mol/kg were chosen for the second round, in which 4×10^4 Monte Carlo cycles including 2×10^4 cycles for equilibration and 2×10^4 cycles for production were executed. In the final round, MOFs with $W_{NH3\_hum} > 0.05$ mol/kg in the second round were selected, in which more than 1×10^5 cycles were implemented until achieving the complete equilibration.

The operational conditions used in this work were listed in Table 1. The temperature and pressure are 298 K and 1 bar, respectively, where the concentration of ammonia is 1000 ppm (i.e. 695.3 μg/L) referred to the breakthrough testing condition in previous work [37]. The RH is 80% with the ratio of $N_2/O_2 = 4{:}1$ in the air. Besides, we also calculated ammonia adsorption performance under dry air conditions for comparing with that under humid air conditions, of which the separation conditions were shown in Table S6. To explore the water and ammonia adsorption behaviors in MOFs, we analyzed gas adsorption density distribution (DD) within typical MOFs by RASPA 2.0 [34], and the potential energy distribution (PED) of a single adsorbate component obtained from PEGrid code [38].

2.3. The evaluation criteria for ammonia capture

In this work, we focused on MOFs with high ammonia uptake for one-off protective equipment used in military activities, in which the high ammonia adsorption capacity (W_{NH3_hum}) is the most important criterion for evaluating the ammonia capture performance of MOFs from the humid air. Besides, the ammonia selectivity over water ($S_{NH3/H2O}$) can be calculated from GCMC simulation according to the following

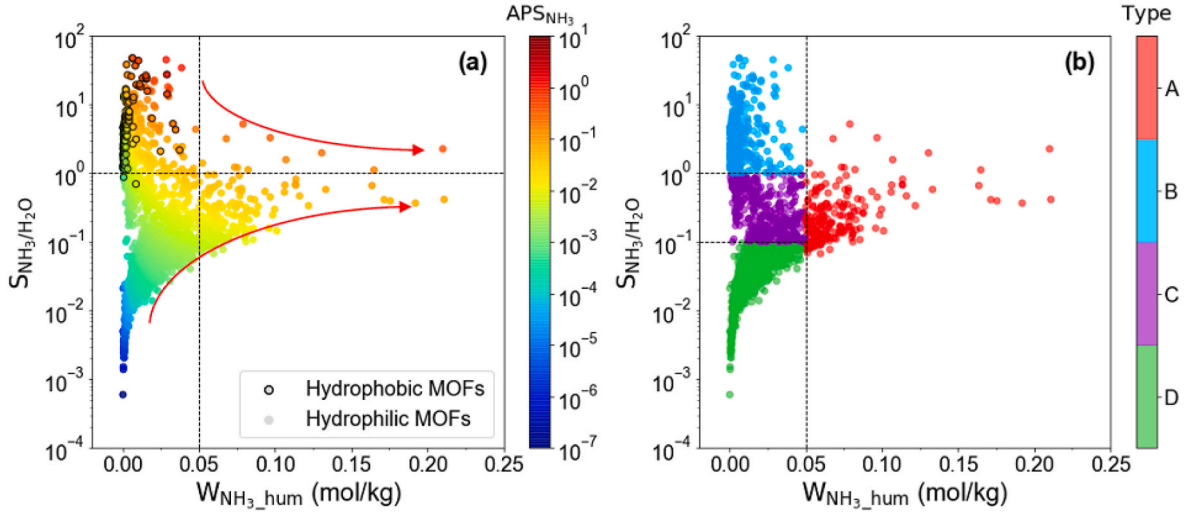

Fig. 2. (a) The relationship between ammonia uptake (W_{NH3_hum}) and ammonia selectivity ($S_{NH3/H2O}$) of 1709 MOFs with highlighted hydrophobic MOFs (125 MOFs) and colored by the adsorbent performance score for ammonia (APS_{NH3}). (b) The classification of MOFs according to W_{NH3_hum} and $S_{NH3/H2O}$.

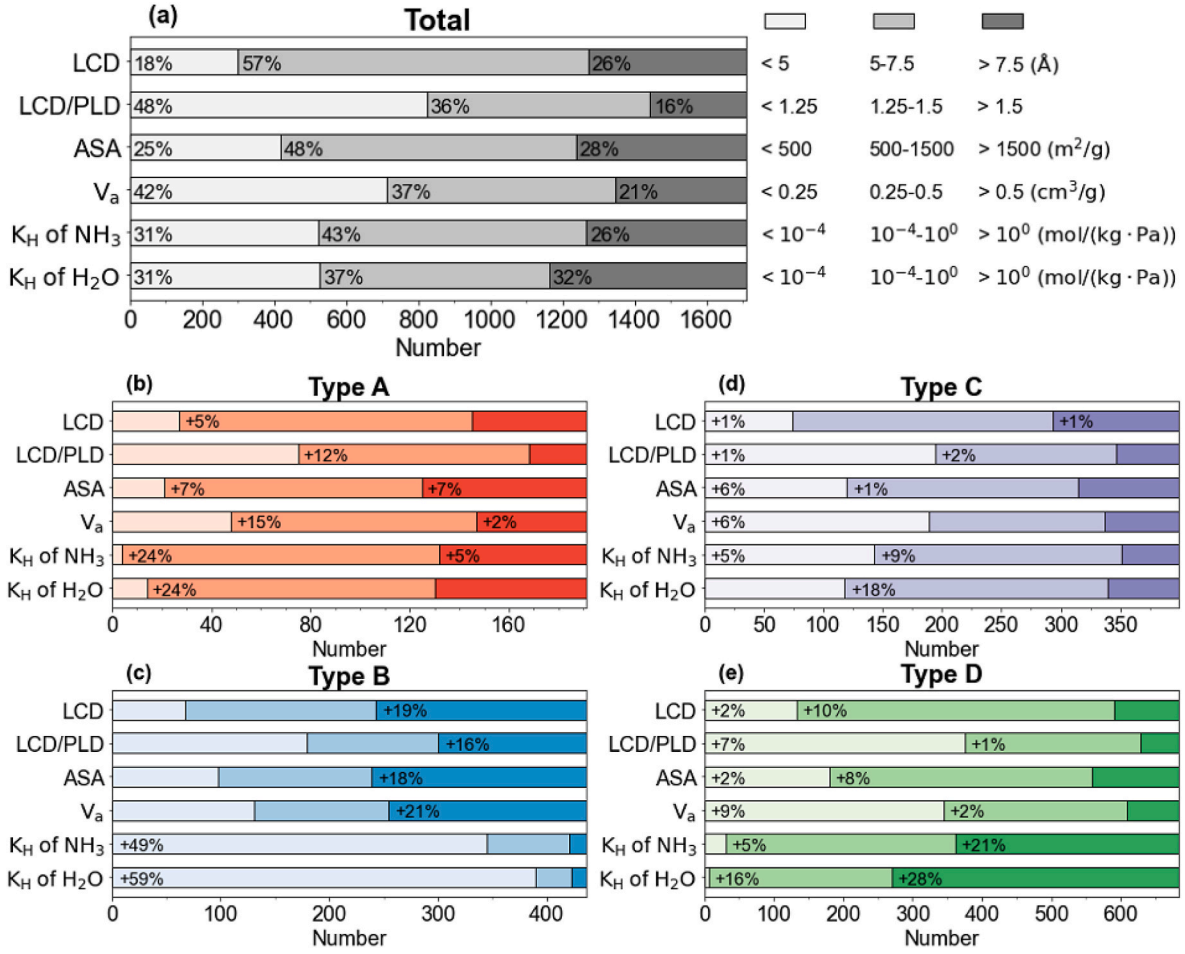

Fig. 3. The distribution of (a) total (b–e) type A-D MOFs in the different ranges of structural characteristics and Henry's constant (K_H). (a) is the percentage of all MOFs with different feature ranges. In (b–e), the "+ percentage" represents the increased percentage of type A-D MOFs in different feature ranges compared with that of total MOFs.

equation.

$$S_{NH3/H2O} = \frac{W_{NH3\_hum}/W_{H2O}}{x_{NH3\_hum}/x_{H2O}} \quad \text{(Eq. 2)}$$

W_{NH3_hum} is the ammonia uptake of MOFs in humid air conditions, W_{H2O} is water uptake, x_{NH3_hum} and x_{H2O} are the mole fraction of ammonia and water in humid air, respectively. Besides, an indicator named adsorbent performance score (APS) [39] was introduced to evaluate the ammonia capture performance. The APS for NH_3 can be obtained according to Eq. (3).

$$APS_{NH3} = W_{NH3\_hum} \times S_{NH3/H2O} \quad \text{(Eq. 3)}$$

The MOFs with both outstanding W_{NH3_hum} and $S_{NH3/H2O}$ usually exhibit high APS_{NH3}, but it should be noticed that the ultra-high $S_{NH3/H2O}$ can also lead to the high APS_{NH3}.

To quantify the influence of competitive water adsorption on ammonia adsorption, the coefficient describing the effects of water adsorption on ammonia uptake (IC_{H2O_NH3}) was defined, which is the percentage of the ratio of the variation in ammonia uptake from humid air (W_{NH3_hum}) and dry air (W_{NH3_dry}) to the ammonia uptake from dry air (W_{NH3_dry}).

$$IC_{H2O\_NH3} = \frac{W_{NH3\_dry} - W_{NH3\_hum}}{W_{NH3\_dry}} \times 100\% \quad \text{(Eq. 4)}$$

$IC_{H2O\_NH3} > 0$ means that the presence of water is unfavorable for ammonia uptake from humid air; conversely, $IC_{H2O\_NH3} < 0$ suggests that the presence of water facilitates ammonia uptake of MOFs from humid air.

3. Results and discussion

3.1. Structure-performance relationship

Fig. 2 showed the adsorption performance including W_{NH3_hum}, $S_{NH3/H2O}$ and APS_{NH3} in the first-round screening. It can be found that all hydrophobic MOFs (K_H of water $< 5 \times 10^{-6}$ mol/(kg.Pa) according to Ref. [25]) exhibit high ammonia selectivity over water ($S_{NH3/H2O}$) but poor ammonia uptake ($W_{NH3\_hum} < 0.05$ mol/kg), which is in line with the conclusion from Moghadam et al. [25]. It also implicates that hydrophobic MOFs are not the potential candidates with satisfactory ammonia uptake of interest. On the other hand, hydrophilic MOFs are favorable for ammonia uptake (Fig. 2a). The reported experimental results [2] in Table S7 demonstrate that the MOFs with high ammonia uptake are hydrophilic with a Henry's constant toward water ($K_{H,water}$) greater than 5×10^{-6} mol/(kg.Pa), validating our predictions. In short, hydrophobic MOFs exhibit higher ammonia selectivity, while hydrophilic MOFs possess higher ammonia uptake. However, not all hydrophilic MOFs present high ammonia uptake according to our simulations. Some hydrophilic MOFs exhibit either ultra-high or ultra-low $S_{NH3/H2O}$ exhibiting low ammonia uptake. In theory, APS_{NH3} that is the product of W_{NH3_hum} and $S_{NH3/H2O}$ can be used to identify the MOFs with high ammonia selectivity and/or ammonia uptake. However, a vast majority of MOFs with high APS_{NH3} exhibit high $S_{NH3/H2O}$ but low W_{NH3_hum} as

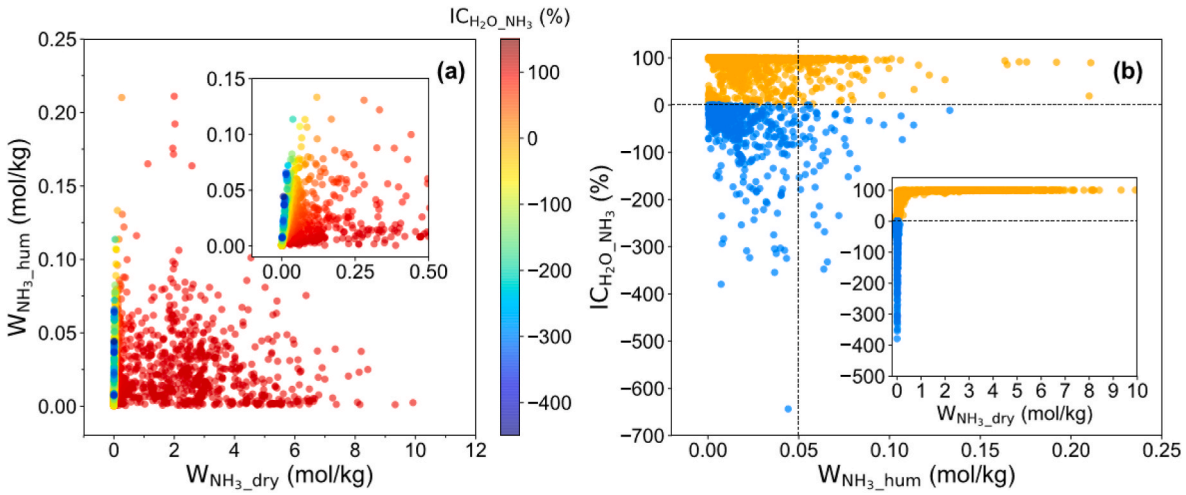

Fig. 4. (a) The ammonia adsorption capacity in humid air (W_{NH3_hum}) and dry air (W_{NH3_dry}) of MOFs colored by IC_{H2O_NH3}. (b) The relationship between W_{NH3_hum}, W_{NH3_dry} and IC_{H2O_NH3}.

demonstrated in Fig. 2a, since $S_{NH3/H2O}$ is several orders of magnitude larger than W_{NH3_hum}. Since the focus of this work is to explore MOFs with high ammonia uptake regardless of selectivity and water adsorption, the high-performing candidates in this work were defined as the ones exhibiting an adsorption capacity of $W_{NH3\_hum} > 0.05$ mol/kg, which was chosen for further study. In order to discriminate the MOFs with different ammonia selectivities and uptakes, we classified them into four categories according to their W_{NH3_hum} and $S_{NH3/H2O}$ in Fig. 2b. According to the classifications, MOFs of type A are of the greatest concern with high W_{NH3_hum} (>0.05 mol/kg) and most of them exhibit moderate $S_{NH3/H2O}$ (0.1–1). MOFs of type B are the ones with the highest $S_{NH3/H2O}$ but low W_{NH3}. MOFs of type C are the ones with both moderate $S_{NH3/H2O}$ and W_{NH3}. MOFs of type D are the ones with both low $S_{NH3/H2O}$ and W_{NH3}. Based on this classification, the SPR between structural characteristics, ammonia/water affinity of MOFs described by K_H and ammonia capture performance was analyzed.

Fig. S1 displays the correlation between ammonia uptake (W_{NH3_hum}) and structure properties as well as ammonia/water affinity, it displays the preferential structure properties or Henry's constants for the top performers with high W_{NH3_hum}. Nonetheless, no obvious distinction of features can be identified for different types of MOFs according to Fig. S1. Therefore, we analyzed the SPR based on the classification in Fig. 3. It can be found that there is no obvious correlation between structural characteristics and ammonia capture performance. In general, most type A MOFs (high W_{NH3_hum}) exhibit tube-like channels (LCD/PLD = 1.25–1.5), moderate LCD (5–7.5 Å), ASA (500–1500 m^2/g) and V_a (0.25–0.5 cm^3/g), and most type B MOFs display large LCD, ASA and V_a, implicating the weak interaction with ammonia and water molecules. Moreover, the K_H of NH_3 and K_H of H_2O representing the affinity of MOFs towards ammonia and water molecules at ultra-low partial pressure respectively can be used to distinguish different types of MOFs. There are obviously more MOFs exhibiting a moderate range of K_H of NH_3 than those of K_H of H_2O in type A MOFs, which are favorable for the high ammonia uptake of type A MOFs. Similar to type A MOFs, more structures exhibit high K_H of NH_3 in type B MOFs, but a majority of type B MOFs display low affinity towards ammonia and water ($<10^{-4}$ mol/(kg·Pa)), leading to their high $S_{NH3/H2O}$. In contrast, in both type C and D MOFs, there are more structures exhibiting high K_H of H_2O than those exhibiting high K_H of NH_3, corresponding to their low $S_{NH3/H2O}$. Whereas a vast majority of type D MOFs exhibit strong affinity towards both ammonia and water, resulting in their lower $S_{NH3/H2O}$ than type C MOFs, most of which exhibit moderate affinity towards both type C and type D MOFs. In short, the affinity of MOFs for ammonia and water plays a more important role in ammonia capture performance than structure characteristics.

Water imposes great impacts on ammonia adsorption in the co-adsorption process, which may inhibit or promote ammonia adsorption performance [2,25,40,41]. To explore the effect of water adsorption on ammonia capture of MOFs, the ammonia adsorption capacity in dry air conditions (W_{NH3_dry}) was also simulated and compared with the ammonia uptake in humid air (W_{NH3_hum}) (Fig. 4a). It is found that there is no clear correlation between the ammonia uptakes in dry and humid

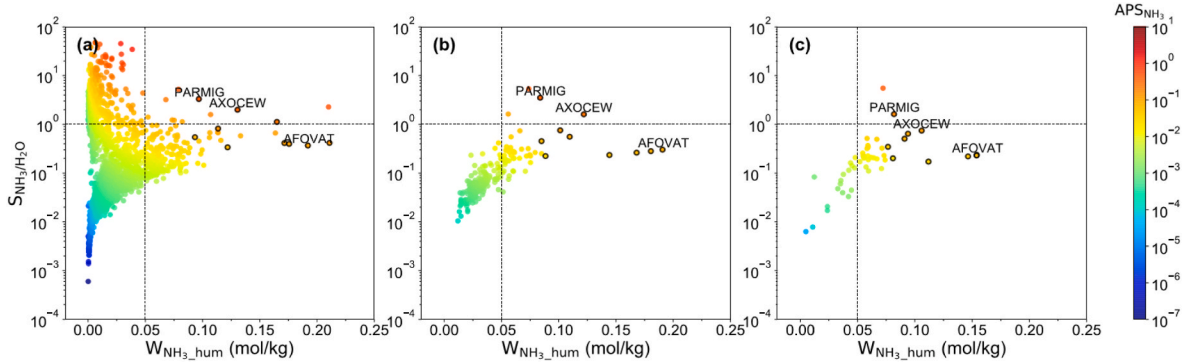

Fig. 5. The relationship between ammonia adsorption capacity (W_{NH3}) and ammonia selectivity ($S_{NH3/H2O}$) in (a) the first round, (b) the second round and (c) the third round screening. The top 10 high-performing MOFs with excellent W_{NH3} after final round are highlighted, among which the ref. code of 3 typical MOFs were marked.

Table 2
The top 10 MOFs ranked by ammonia adsorption capacity (W_{NH3_hum}) according to the third-round screening.

Rank	Ref. code	Molecular formula	LCD (Å)	ASA (m^2/g)	V_a (cm^3/g)	K_H of NH_3 (mol/(kg.Pa))	K_H of H_2O (mol/(kg.Pa))	W_{NH3_hum} (mol/kg)	W_{H2O} (mol/kg)	$S_{NH3/H2O}$
1	AFOVAT	$LaH_{12}(C_7O_2)_3$	8.329	1462	0.455	1.15×10^3	1.27×10^4	0.154	24.472	0.237
2	AFOVOH	$NdH_{12}(C_7O_2)_3$	8.788	1442	0.462	7.60×10^2	4.88×10^4	0.154	25.242	0.229
3	AFOTUL	$SmH_{12}(C_7O_2)_3$	8.802	1446	0.460	1.18×10^4	1.24×10^5	0.146	25.086	0.219
4	AFOVIB	$GdH_{12}(C_7O_2)_3$	8.793	1379	0.440	7.87×10^1	4.44×10^2	0.112	24.515	0.172
5	AXOCEW	$ZnH_8C_{17}(O_2F_3)_2$	7.560	1025	0.305	2.44×10^{-2}	2.50×10^{-2}	0.106	5.367	0.742
6	TEDLUK	$ZnH_{15}C_{18}N_3O_5$	5.529	366	0.117	8.36×10^{-4}	1.01×10^{-4}	0.094	5.521	0.640
7	PUMNIV	$CdHgC_4(SN)_4$	5.720	718	0.235	2.82×10^{-1}	1.80×10^{-1}	0.091	6.783	0.505
8	PARMIG	$NiH_{10}C_{16}(NO)_4$	4.625	402	0.190	4.19×10^{-4}	1.78×10^{-5}	0.082	1.909	1.613
9	LUFNEG	$MnH_{10}C_{14}(NO_2)_2$	4.766	1048	0.250	2.02×10^{-3}	8.28×10^{-4}	0.081	15.163	0.201
10	WENDIE	$ZnH_4C_8(N_2O)_2$	4.915	512	0.196	6.76×10^2	7.68×10^2	0.077	8.336	0.345

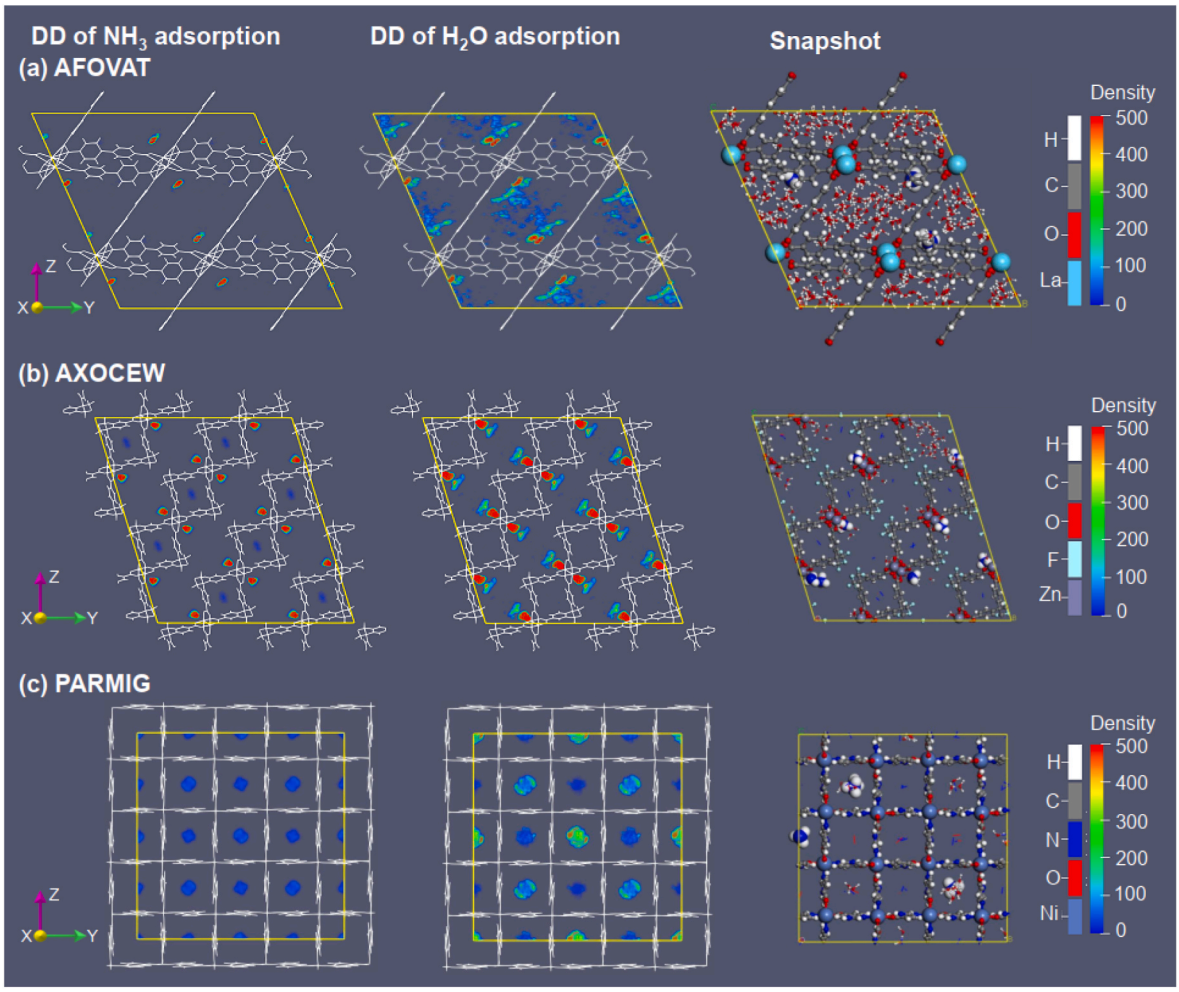

Fig. 6. The density distribution (DD) maps of ammonia and water adsorption, and the snapshot in the simulation of (a) AFOVAT, (b) AXOCEW and (c) PARMIG.

air, implicating that water in atmosphere imposes complicated impacts on ammonia adsorption from air. In order to quantify such impacts, we introduced the coefficient describing the impacts of water on ammonia uptake (IC_{H2O_NH3}) as defined in Eq. (4). $IC_{H2O\_NH3} > 0$ indicates the decreased ammonia uptake from humid air compared with that from dry air, and $IC_{H2O\_NH3} < 0$ suggests the enhanced ammonia uptake from humid air compared with that from dry air. Most MOFs exhibit $IC_{H2O\_NH3} > 0$ and higher W_{NH3_hum} than MOFs with $IC_{H2O\_NH3} < 0$, indicating that although the presence of water reduces ammonia uptake of some MOFs from air, their ammonia uptake is still higher than that with $IC_{H2O\_NH3} < 0$. Besides, IC_{H2O_NH3} of most type A MOFs (i.e. $W_{NH3\_hum} > 0.05$ mol/kg) are positive, suggesting that water inhibits ammonia adsorption in those top-performing MOFs. In addition, we found that MOFs with $IC_{H2O\_NH3} < 0$ exhibit both lower K_H of NH_3 and K_H of H_2O than MOFs with positive IC_{H2O_NH3}, but there is no correlation between structural characteristics and IC_{H2O_NH3} (in Fig. S2). Besides, previous study [2] reported that the ammonia uptakes of most MOFs were increased with water uptake at humid conditions. However, dissimilarly, the dependence of ammonia uptake (W_{NH3_hum}) on water uptake (W_{H2O}) from humid air was not observed (Fig. S3), which may be due to the vast number of MOFs investigated in this work.

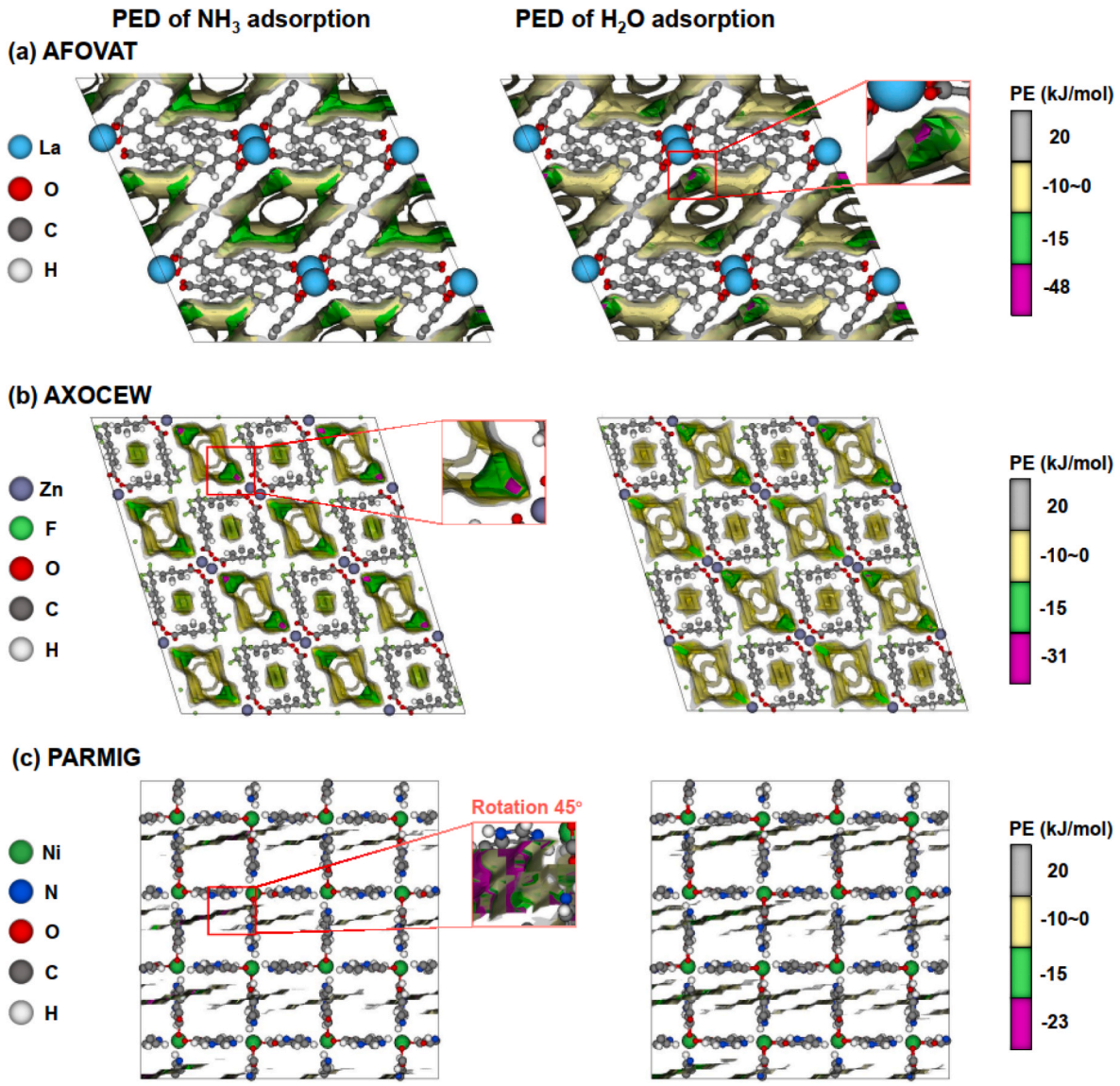

Fig. 7. The potential energy distribution (PED) maps of ammonia and water adsorption of (a) AFOVAT, (b) AXOCEW and (c) PARMIG. The color map represents the intensity potential energy (PE), and the purple area is the strongest adsorption site. (For interpretation of the references to color in this figure legend, the reader is referred to the Web version of this article.)

3.2. *High-performing MOFs after screening*

According to the criterion of $W_{NH3\_hum} > 0.05$ mol/kg, the number of selected MOFs from the first, second and third round is 1709, 191 and 50, respectively (Fig. 5). The detailed screening details were provided in Tables S2–S4. With the progress of screening from the first round to the last round, the number of MOFs with $W_{NH3\_hum} > 0.05$ mol/kg is gradually decreased, and there are only 34 MOFs with $W_{NH3\_hum} > 0.05$ mol/kg finally due to the extended MC cycles that gives rise to the more accurate prediction on ammonia capture performance. MOFs with outstanding ammonia uptake deserve special attention, and the top 10 MOFs exhibiting the largest W_{NH3_hum} from the final round of screening are presented in Table 2. Five MOFs show $W_{NH3} > 0.1$ mol/kg of W_{NH3}, among which the top four MOFs (i.e. AFOVAT, AFOVOH, AFOTUL and AFOVIB) with similar adsorption performance and structure characteristics possess similar structures differing only in their metal sites. It is worth noting that $S_{NH3/H2O}$ of most MOFs is less than 1, only PARMIG (ranked No. 8) exhibits $S_{NH3/H2O}$ of 1.6, which is mainly affected by the amount of W_{H2O} under similar W_{NH3_hum}. These top 10 MOFs can be classified into three classes according to the amount of W_{H2O} (i.e. high $W_{H2O} > 15$ mol/kg, medium $W_{H2O} = 5$–15 mol/kg and low $W_{H2O} < 5$ mol/kg). Therefore, three typical high-performing MOFs with high W_{NH3_hum} and different W_{H2O}, i.e., AFOVOH (No.1), AXOCEW (No.5) and PARMIG (No.8) are chosen for further analysis to explore their water and ammonia adsorption behaviors.

The ammonia and water density distribution (DD) maps and snapshots of selected MOFs in Fig. 6 demonstrate that ammonia and water molecules are mainly adsorbed around metal sites in AFOVAT and AXOCEW, while gas molecules are located in the center of pores of PARMIG, which may be caused by its strong interaction resulting from overlapped well depth in its small pore size. The low density of ammonia molecules in the center of small pores (about 5 Å) is observed in AXOCEW, and water molecules are only adsorbed in its large pores (>7 Å) due to a larger dynamic diameter of water than ammonia. In the snapshots, in line with the results of W_{H2O}, a lot of water molecules fill the pores of AFOVAT, some water molecules are distributed near the metal sites and in the pores of AXOCEW, and few water molecules are present in PARMIG. The states of ammonia and water adsorption are in line with DD maps, except for the ammonia molecules that are adsorbed near the linkers instead of metal sites in AFOVAT. It may be caused by a large

number of water molecules competing with ammonia molecules for the adsorption sites, which is elucidated from the view of adsorption potential energy (see Fig. 7).

In PED, it is noted that the negative value of potential energy represents the attractive interaction between frameworks and adsorbate molecules, and the greater absolute value indicates the stronger interaction. Similar PED of ammonia and water adsorption suggests their competitive adsorption. Water molecules preferentially adsorb on metal sites than ammonia molecules due to the stronger interaction between water and metal sites as indicated by the PED (the purple area) of AFOVAT. Since the high W_{H2O} of AFOVAT, a lot of water molecules occupy the metal sites, thus the ammonia molecules only adsorb near the linkers (the green area that secondary adsorbed area). Then, there is a larger number of water molecules filling the pore of MOFs (the weaker adsorbed area colored by yellow). In contrast with AFOVAT, the PE of ammonia is higher than that of water in AXOCEW and PARMIG, indicating that ammonia molecules preferentially adsorbed than water in these MOFs.

4. Conclusions

In this work, in order to identify high-performing MOFs with satisfactory ammonia uptake from humid air, 2932 CoRE MOFs were assessed by high-throughput computational screening based on GCMC simulation regardless of their hydrophilicity. It is found that although all hydrophobic MOFs exhibit high ammonia selectivity over water, hydrophilic MOFs possess higher ammonia uptake than hydrophobic ones. Classification of MOFs based on both their ammonia uptake and selectivity demonstrate that Henry's constants of MOFs towards ammonia and water play a more important role in determining ammonia capture performance from humid air. There are more type A MOFs exhibiting moderate K_H of NH_3 than that of K_H of H_2O, leading to their high ammonia uptake. In contrast, a larger number of type B MOFs exhibit low K_H of H_2O than K_H of NH_3, resulting in their ultrahigh $S_{NH3/H2O}$. The coefficient describing the impacts of water adsorption on ammonia uptake (IC_{H2O_NH3}) demonstrated that the presence of water in humid air is able to either promote ($IC_{H2O\_NH3} < 0$) or reduce ($IC_{H2O\_NH3} > 0$) ammonia uptake of MOFs, and the ones with $IC_{H2O\_NH3} > 0$ possess higher ammonia uptake, which may be ascribed to their high affinity towards ammonia. 34 MOFs with $W_{NH3\_hum} > 0.05$ mol/kg and five MOFs with $W_{NH3\_hum} > 0.1$ mol/kg were obtained after three-round screening. It should be noted that the dependence of W_{NH3_hum} on water uptake from humid air was not observed in this work, which may be due to the large number and diversity of MOFs investigated in this work. Based on the analysis of top-performing MOFs from screening, the competitive adsorption between ammonia and water is demonstrated by the similar density and potential energy distribution of ammonia and water adsorption in frameworks, implicating similar adsorption sites for ammonia and water molecules. These findings obtained in this work not only help to deeply understand the ammonia adsorption behaviors in humid air but also guide the exploration of MOF adsorbents for efficiently capturing ammonia from humid air.

CRediT authorship contribution statement

Zhilu Liu: Writing – original draft, Investigation, Data curation. **Xinbo Wang:** Conceptualization, Data curation, Methodology, Writing – original draft. **Yuexin Liu:** Investigation, Data curation. **Li Li:** Conceptualization, Funding acquisition, Writing – review & editing. **Song Li:** Writing – review & editing, Supervision, Project administration, Methodology, Conceptualization.

Declaration of competing interest

The authors declare that they have no known competing financial interests or personal relationships that could have appeared to influence the work reported in this paper.

Acknowledgments

This work was supported by National Natural Science Foundation of China (No. 21876204), Foundation of State Key Laboratory of NBC Protection for Civilian, China (No. SKLNBC2018 04). The computation was carried out at National Supercomputer Center in Shenzhen.

Appendix A. Supplementary data

Supplementary data to this article can be found online at https://doi.org/10.1016/j.micromeso.2021.111659.

References

[1] Y. Chen, Y. Wang, C. Yang, S. Wang, J. Yang, J. Li, Antenna-protected metal–organic squares for water/ammonia uptake with excellent stability and regenerability, ACS Sustain. Chem. Eng. 5 (6) (2017) 5082–5089.
[2] Y. Khabzina, D. Farrusseng, Unravelling ammonia adsorption mechanisms of adsorbents in humid conditions, Microporous Mesoporous Mater. 265 (2018) 143–148.
[3] G. Han, C. Liu, Q. Yang, D. Liu, C. Zhong, Construction of stable IL@MOF composite with multiple adsorption sites for efficient ammonia capture from dry and humid conditions, Chem. Eng. J. 401 (2020) 126106.
[4] K. Vikrant, V. Kumar, K.-H. Kim, D. Kukkar, Metal–organic frameworks (MOFs): potential and challenges for capture and abatement of ammonia, J. Mater. Chem. A 5 (44) (2017) 22877–22896.
[5] H. Jasuja, G.W. Peterson, J.B. Decoste, M.A. Browe, K.S. Walton, Evaluation of MOFs for air purification and air quality control applications: ammonia removal from air, Chem. Eng. Sci. 124 (2015) 118–124.
[6] D.J. Tranchemontagne, J.L. Mendoza-Cortes, M. O'Keeffe, O.M. Yaghi, Secondary building units, nets and bonding in the chemistry of metal-organic frameworks, Chem. Soc. Rev. 38 (5) (2009) 1257–1283.
[7] H. Furukawa, N. Ko, Y.B. Go, N. Aratani, S.B. Choi, E. Choi, A.O. Yazaydin, R. Q. Snurr, M. O'Keeffe, J. Kim, O.M. Yaghi, Ultrahigh porosity in metal-organic frameworks, Science 329 (5990) (2010) 424–428.
[8] O.K. Farha, I. Eryazici, N.C. Jeong, B.G. Hauser, C.E. Wilmer, A.A. Sarjeant, R. Q. Snurr, S.T. Nguyen, A.O. Yazaydin, J.T. Hupp, Metal-organic framework materials with ultrahigh surface areas: is the sky the limit? J. Am. Chem. Soc. 134 (36) (2012) 15016–15021.
[9] N. Liu, J. Wang, M. Tian, J. Lei, J. Wang, W. Shi, X. Zhang, L. Tang, Boron nitride nanosheets decorated MIL-53 (Fe) for efficient synergistic Ibuprofen photocatalytic degradation by persulfate activation, J. Colloid Interface Sci. 603 (2021) 270–281.
[10] Y. Wang, F. Bi, Y. Wang, M. Jia, X. Tao, Y. Jin, X. Zhang, MOF-derived CeO2 supported Ag catalysts for toluene oxidation: the effect of synthesis method, Mol. Catal. 515 (2021) 111922.
[11] X. Zhang, X. Shi, Q. Zhao, Y. Li, J. Wang, Y. Yang, F. Bi, J. Xu, N. Liu, Defects controlled by acid-modulators and water molecules enabled UiO-67 for exceptional toluene uptakes: an experimental and theoretical study, Chem. Eng. J. 427 (2022) 131573.
[12] S. Kitagawa, R. Kitaura, S. Noro, Functional porous coordination polymers, Angew. Chem. Int. Ed. 43 (18) (2004) 2334–2375.
[13] W. Morris, C.J. Doonan, O.M. Yaghi, Postsynthetic modification of a metal-organic framework for stabilization of a hemiaminal and ammonia uptake, Inorg. Chem. 50 (15) (2011) 6853–6855.
[14] Y. Chen, X. Zhang, K. Ma, Z. Chen, X. Wang, J. Knapp, S. Alayoglu, F. Wang, Q. Xia, Z. Li, T. Islamoglu, O.K. Farha, Zirconium-based metal–organic framework with 9-connected nodes for ammonia capture, ACS Appl. Nano Mater. 2 (10) (2019) 6098–6102.
[15] A.J. Rieth, Y. Tulchinsky, M. Dinca, High and reversible ammonia uptake in mesoporous azolate metal-organic frameworks with open Mn, Co, and Ni sites, J. Am. Chem. Soc. 138 (30) (2016) 9401–9404.
[16] A.J. Rieth, M. Dinca, Controlled gas uptake in metal-organic frameworks with record ammonia sorption, J. Am. Chem. Soc. 140 (9) (2018) 3461–3466.
[17] D.W. Kim, D.W. Kang, M. Kang, J.H. Lee, J.H. Choe, Y.S. Chae, D.S. Choi, H. Yun, C.S. Hong, High ammonia uptake of a metal-organic framework adsorbent in a wide pressure range, Angew Chem. Int. Ed. Engl. 59 (50) (2020) 22531–22536.
[18] N. Nijem, K. Fürsich, H. Bluhm, S.R. Leone, M.K. Gilles, Ammonia adsorption and Co-adsorption with water in HKUST-1: spectroscopic evidence for cooperative interactions, J. Phys. Chem. C 119 (44) (2015) 24781–24788.
[19] J.B. DeCoste, M.S. Denny Jr., G.W. Peterson, J.J. Mahle, S.M. Cohen, Enhanced aging properties of HKUST-1 in hydrophobic mixed-matrix membranes for ammonia adsorption, Chem. Sci. 7 (4) (2016) 2711–2716.
[20] G.W. Peterson, G.W. Wagner, A. Balboa, J. Mahle, T. Sewell, C.J. Karwacki, Ammonia vapor removal by Cu-3(BTC)(2) and its characterization by MAS NMR, J. Phys. Chem. C 113 (31) (2009) 13906–13917.
[21] T. Grant Glover, G.W. Peterson, B.J. Schindler, D. Britt, O. Yaghi, MOF-74 building unit has a direct impact on toxic gas adsorption, Chem. Eng. Sci. 66 (2) (2011) 163–170.

[22] M.J. Katz, A.J. Howarth, P.Z. Moghadam, J.B. DeCoste, R.Q. Snurr, J.T. Hupp, O. K. Farha, High volumetric uptake of ammonia using Cu-MOF-74/Cu-CPO-27, Dalton Trans. 45 (10) (2016) 4150–4153.
[23] Y.J. Colon, R.Q. Snurr, High-throughput computational screening of metal-organic frameworks, Chem. Soc. Rev. 43 (16) (2014) 5735–5749.
[24] Z. Liu, W. Li, H. Liu, X. Zhuang, S. Li, Research progress of high-throughput computational screening of metal-organic frameworks, Acta Chim. Sinica 77 (4) (2019) 323–339.
[25] P.Z. Moghadam, D. Fairen-Jimenez, R.Q. Snurr, Efficient identification of hydrophobic MOFs: application in the capture of toxic industrial chemicals, J. Mater. Chem. A 4 (2) (2016) 529–536.
[26] D. Nazarian, J.S. Camp, D.S. Sholl, A comprehensive set of high-quality point charges for simulations of metal–organic frameworks, Chem. Mater. 28 (3) (2016) 785–793.
[27] C. Altintas, G. Avci, H. Daglar, A. Nemati Vesali Azar, I. Erucar, S. Velioglu, S. Keskin, An extensive comparative analysis of two MOF databases: high-throughput screening of computation-ready MOFs for CH4 and H2 adsorption, J. Mater. Chem. A 7 (16) (2019) 9593–9608.
[28] W. Li, X. Xia, M. Cao, S. Li, Structure–property relationship of metal–organic frameworks for alcohol-based adsorption-driven heat pumps via high-throughput computational screening, J. Mater. Chem. A 7 (13) (2019) 7470–7479.
[29] Z.W. Qiao, Q.S. Xu, J.W. Jiang, Computational screening of hydrophobic metal–organic frameworks for the separation of H2S and CO2 from natural gas, J. Mater. Chem. A 6 (39) (2018) 18898–18905.
[30] C. Altintas, S. Keskin, Role of partial charge assignment methods in high-throughput screening of MOF adsorbents and membranes for CO2/CH4 separation, Mol. Syst. Des. Eng. 5 (2) (2020) 532–543.
[31] W. Li, Z. Rao, Y.G. Chung, S. Li, The role of partial atomic charge assignment methods on the computational screening of metal-organic frameworks for CO2 capture under humid conditions, ChemistrySelect 2 (29) (2017) 9458–9465.
[32] T.A. Manz, D.S. Sholl, Chemically meaningful atomic charges that reproduce the electrostatic potential in periodic and nonperiodic materials, J. Chem. Theor. Comput. 6 (8) (2010) 2455–2468.
[33] T.F. Willems, C.H. Rycroft, M. Kazi, J.C. Meza, M. Haranczyk, Algorithms and tools for high-throughput geometry-based analysis of crystalline porous materials, Microporous Mesoporous Mater. 149 (1) (2012) 134–141.
[34] D. Dubbeldam, S. Calero, D.E. Ellis, R.Q. Snurr, RASPA: molecular simulation software for adsorption and diffusion in flexible nanoporous materials, Mol. Simulat. 42 (2) (2015) 81–101.
[35] A.K. Rappi, C.J. Casewit, K.S. Colwell, W.A. Goddard, W.M. Skid, UFF, a full periodic table force field for molecular mechanics and molecular dynamics simulations, J. Am. Chem. Soc. 114 (25) (1992) 10024–10035.
[36] Transferable Potentials for Phase Equilibria Force Field, 2020. http://trappe.oit.umn.edu.
[37] G.W. Peterson, J.B. DeCoste, T.G. Glover, Y. Huang, H. Jasuja, K.S. Walton, Effects of pelletization pressure on the physical and chemical properties of the metal–organic frameworks Cu3(BTC)2 and UiO-66, Microporous Mesoporous Mater. 179 (2013) 48–53.
[38] PEGrid, 2015. https://github.com/michelleliu/PEGrid.
[39] Y.G. Chung, D.A. Gomez-Gualdron, P. Li, K.T. Leperi, P. Deria, H.D. Zhang, N. A. Vermeulen, J.F. Stoddart, F.Q. You, J.T. Hupp, O.K. Farha, R.Q. Snurr, In silico discovery of metal-organic frameworks for precombustion CO2 capture using a genetic algorithm, Sci. Adv. 2 (10) (2016), e1600909.
[40] J.M. Kolle, M. Fayaz, A. Sayari, Understanding the effect of water on CO2 adsorption, Chem. Rev. 121 (13) (2021) 7280–7345.
[41] J. Rogacka, A. Seremak, A. Luna-Triguero, F. Formalik, I. Matito-Martos, L. Firlej, S. Calero, B. Kuchta, High-throughput screening of metal – organic frameworks for CO2 and CH4 separation in the presence of water, Chem. Eng. J. 403 (2021) 126392.